

MODELLING SNOW MELT PROCESSES IN ALPINE AREAS

Josef JANSA¹, Karl KRAUS¹, Günter BLÖSCHL², Robert KIRNBAUER², Gerhard KUSCHNIG³

¹Institute of Photogrammetry and Remote Sensing (I.P.F.), Vienna University of Technology, Austria

²Institute of Hydraulics, Hydrology and Water Resources Management (IHGW), Vienna University of Technology

³Department of Water Management (MA31), Vienna City Council, Austria

Josef.Jansa@tuwien.ac.at; Guenter.Bloeschl@tuwien.ac.at

Working Group IC-23

KEY WORDS: Modelling, Sustainability, Multi-temporal

ABSTRACT

The Water Supply Department of the Vienna City Council (MA31) operates a number of water supply catchments in a Karstic region of the Alps some 80 km south west of Vienna where the springs are fed by snow melt water during a substantial part of the year. To better understand and ultimately predict the space-time patterns of melt water, MA31 initiated a research initiative which is the subject of this paper. We set up a hydrological snow accumulation and melt model based on the 20 m grid of the DTM which simulates the energy balance components at the snow surface and the coupled heat and mass flow within the snowpack for each grid element. The snow model is driven by meteorological observations at an hourly time step. Some of the model parameters of the snow model need to be calibrated and we did that by comparing snow cover patterns (snow/no snow) simulated by the snow model with snow cover patterns derived from the SPOT based snow classification. This comparison enabled us to find reliable model parameters. The snow model can be used to simulate, among other things, the space-time patterns of snow water equivalent and snow melt within the study domain. The snow model still needs some refinement and ultimately we are planning to combine the model with an operational forecasting procedure.

KURZFASSUNG

Die Wiener Wasserwerke (MA31) betreiben eine Reihe von Quelleinzugsgebieten für die Trinkwasserversorgung in einem Karstgebiet in den Kalkvorbergen etwa 80km südwestlich von Wien, in denen Schneeschmelze wesentlich zum Abfluß beiträgt. Um die raum-zeitliche Verteilung der Schneeschmelze in diesen Gebieten besser zu verstehen und letztendlich vorherzusagen, initiierte die MA31 ein Forschungsprojekt, von dem erste Ergebnisse in dieser Arbeit vorgestellt werden. Es wurde ein Schneeschmelz- und Akkumulationsmodell auf Basis des DGM Rasters für das Untersuchungsgebiet aufgestellt, das für jedes Rasterelement die Energiebilanz und die Prozesse innerhalb der Schneedecke simuliert. Das Modell verwendet als Eingangsgrößen stündliche meteorologische Daten. Einige der Modellparameter des Schneemodells müssen geeicht werden, und dies wurde durch einen Vergleich von mit dem Schneemodell simulierten Schneebedeckungsmustern mit aus den SPOT Bildern abgeleiteten Schneebedeckungsmustern ermöglicht. Die Eichung ergab einen Modellparametersatz, der zuverlässige Schneesimulationen für das Untersuchungsgebiet erlaubt. Insbesondere kann der Schneewasserwert und die Schneeschmelze mit einer hohen räumlichen und zeitlichen Auflösung berechnet werden. Gewisse Verfeinerungen des Schneemodells sind noch nötig, und es ist auch geplant, das Modell in ein operationelles Vorhersagesystem einzubinden.

1 INTRODUCTORY NOTES

In 1997 the Water Supply Department of the Vienna City Council (MA31) proposed a research initiative to investigate the amount and timing of water that is delivered from the seasonal snow cover to the springs in one of their major water supply catchments. The springs are located in a Karstic region of the Alps some 80 km south west of Vienna. The area under investigation in this pilot project covers some 80 km² with terrain elevations ranging from 700 m to 1900 m a.s.l. The main mountain in the area is the Schneeealpe which has a marked plateau at 1700m elevation. Typically, the snow cover period lasts from October to June, and melting occurs in a number of episodes from late February to early June.

Because of the importance to the city administration of understanding the snow melt processes in this area, they provided funds for buying satellite imagery and for making in situ observations of meteorological variables and snow properties (i.e. snow courses). Additional funding was provided by the Austrian Federal Ministry of Science and Transport. The project was scheduled to examine three snow melt periods from spring 1998 to spring 2000. The first two years have been dedicated to acquiring background data and to developing and calibrating the snow model. The

third year will be used for fine tuning the observational procedures and for validating the snow model. In addition, ESA provided ERS SAR data for the 1999 snow melt period as part of their third Announcement of Opportunity.

The scientific partners of the project are the Institute of Hydraulics, Hydrology and Water Resources Management (IHGW) and the Institute of Photogrammetry and Remote Sensing (I.P.F.), both at the Vienna University of Technology. IHGW has a long experience with hydrological snow models (Blöschl et al., 1991). The I.P.F. has been responsible for the overall project management as well as for the photogrammetric tasks of generating a detailed digital terrain model (DTM), performing the land cover classification and the satellite image compilations including parametric geometric rectification and snow classification. The interest of the Vienna Water Supply Department resides in understanding snow processes and, ultimately, in obtaining a mathematical model that is able to forecast melt water production.

2 PREPARATORY WORK

As an input to the snow model a range of data are needed. These include data that only change slowly with time or are time invariant and data that change quickly with time. The former include terrain properties and the land cover while the latter include snow related data and meteorological data. In a preparatory phase of the project we acquired terrain and land cover related information which can be used throughout an extended project period.

2.1 The Digital Terrain Model and Derived Properties

Great effort has been spent on the derivation of the terrain model (Figure 1). Aerial photographs at a scale of 1:15000 have been digitised in order to derive a 20 m DTM grid with additional breaklines and formlines which are very important in areas with significant slope discontinuities, such as rugged rock formations, escarpments and cliffs as well as dolines which are typical Karst features in the study area. We then derived terrain slope and curvature and the local horizon from the DTM. The local horizon is equivalent to the so-called sky plot used in GPS planning and has been obtained by calculating, for each grid position in the DTM, the zenith angle to the horizon for a predefined number of azimuth positions. If eight uniformly spaced azimuth directions (0° , 45° , 90° , ..., 270° , 315°) are selected, the local horizon data set consists of an eight layer multiband image, each band containing the zenith angles for one azimuth. All terrain processing has been carried out by the program package SCOP which has been developed at I.P.F. in close cooperation with INPHO Stuttgart (I.P.F., 1999). All time variant variables related to terrain (e.g. incident angles that depend on the solar position) have been calculated in the snow model described below.



Figure 1: shaded DTM

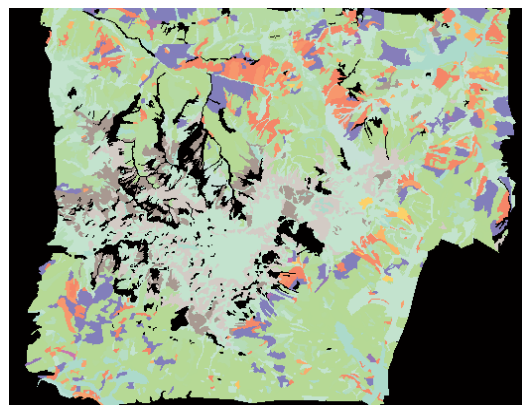


Figure 2: Land Cover

2.2 The Land Cover Classification

Since land cover plays an important role in snow accumulation and depletion a detailed classification was carried out based on visual photo interpretations in CIR aerial photographs (1:15000). Not only did we distinguish individual species but also different tree heights and stand densities. This gave a total of 33 land cover classes (Figure 2). For example, red in Figure 2 relates to dense beech forest while light red/orange relates to a low density beech forest. We assumed that over the period of this study of a number of years, land cover does not change significantly. Other parameters that would have been of interest are soil properties and the hydrogeology of the area. It is much more difficult to map these parameters. Because of this, the current study is limited to understanding and estimating the space-time patterns of melt water production at the base of the snow pack. Future studies will examine the subsurface flow paths of this melt water.

3 SATELLITE IMAGERY

3.1 Utilisation of Satellite Images

Although the final snow model, ideally, should only need meteorological observations as an input, it is essential to calibrate and validate the model with additional observations that are distributed in space. One of the outputs of the snow model are the snow cover patterns as a function of time, i.e. the spatial patterns of whether there was snow/no snow on the ground. These patterns can be checked against snow cover patterns derived from snow cover classifications based on satellite images. This comparison allows a model test with completely independent data. Snow cover related information can be derived from a number of different satellite sensors. An obvious choice are optical satellite images. As a result of a SPOT programming request, four multispectral scenes per spring period could be captured in the past two project years. Figure 3 shows the images for the year 1998. Other optical images were not available from the standard archives because of prevailing bad weather conditions during the crucial season in the area of interest. A possible alternative is SAR imagery which can provide information on the wetness of the snow.

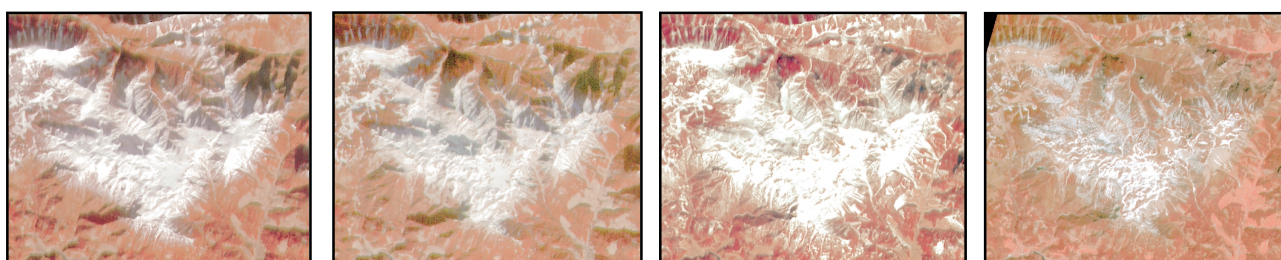


Figure 3: SPOT XS images of 18 February, 20 February, 31 March and 8 May 1998 (© Spot Image France)

3.2 Snow Classification

Although, at first sight, classifying snow seems to be straightforward, it turned out to be difficult for the current project objectives. Winther (1999) describes snow classification with Landsat TM data and concludes that a mid-infrared (MIR) channel is very helpful for class discrimination. In our case the MIR band was not available (up to now only three pictures have been acquired by SPOT4, all others are pure SPOT XS data). Other problems were caused by vegetation and terrain shape. Not only is a part of the study area densely vegetated and the topography is rugged but also are we interested in the snow on the ground rather than on top of the vegetation. A first attempt involved common multispectral classification algorithms, such as supervised Maximum Likelihood or unsupervised Isodata technique (Iterative Self-Organizing Data Analysis Technique, Jensen, 1996), which were applied to the whole image. The classification results, as compared to ground truth, were not satisfactory. However, with a slight modification of the processing chain, the result could be improved significantly. First, the image was segmented into subimages defined by classes of light incidence angles. Then, the standard classification algorithms were applied to each subimage independently, thus reducing the number of classes per run and facilitating the class discrimination. The final classification was then obtained by merging the subimages.

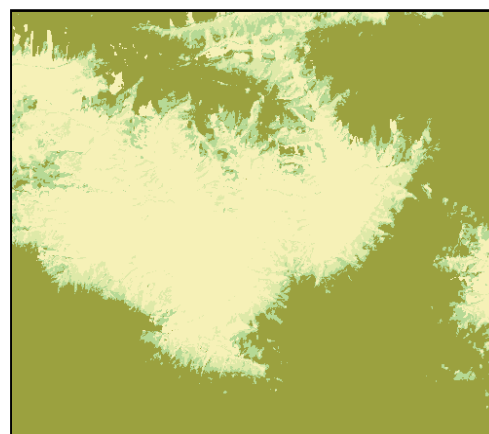


Figure 4: Snow Classes

Finally, four snow cover classes could be clearly distinguished: *Full snow cover* (full snow cover and no terrain discernable); *Snow* (snow clearly visible although soil or vegetation is discernable); *Patchy snow* (not much snow visible, soil or vegetation can be clearly recognized); *No snow* (no snow visible). Please note the terms “visible” and “discernable” implying that the *No snow* class is likely to be identified in densely vegetated areas with a deep snow pack if the tree tops are snow free. Figure 4 shows an example (18 February 1998) with the above mentioned four classes coded as yellow, light green, green and dark green representing full snow cover, snow, patchy snow and no snow, respectively. However, as mentioned above, this multispectral classification does not provide information on the snow depth.

3.3 Interpretation of ERS SAR Images

The great advantage of SAR images is their independence of bad weather conditions. Therefore, they are optimally suited for observation in areas and/or periods of frequent cloud cover. Statistical analysis of the “Schneealpe” region

with data retrieved from the NOAA AVHRR image archive disclosed that only few days per month may be expected cloudless, thus suggesting that SAR images might be appropriate also for this project. SAR images have already been used for classification of (mainly the wetness) of snow and/or determination of snow patterns in the past (e.g. Nagler et al., 1998, Caves et al., 1999). In mountainous areas severe shadow, layover and foreshortening effects deteriorate the quality of images, making a complete compilation from one image impossible. In practice two images, an ascending and a descending one, are merged hoping that areas with radiometric problems in one image can be replaced by the partner image. ERS SAR PRI images have been provided by ESA for the project in 1999. However, due to ESA's programming strategy, which uses the ascending path for data acquisition by the competing wind scatterometer, not all ordered ascending images were available. Eventually three image pairs and two single images have been delivered. The descending images have been taken at 9:00 a.m. and the ascending one at 9:00 p.m. on the same day. The acquisition dates were 11 Feb.(asc and desc), 18 March (asc and desc), 22 April (desc), 27 May (asc and desc) and 1 July 1999 (desc).

As exact absolute radiometric modelling of SAR images is rather complex and acceptable accuracy depends essentially on many parameters that are usually either not available (scattering coefficient of terrain surface and surface cover) or known not precisely enough (terrain shape and slopes), the common procedures are based on relative compilations by calculating the ratio between the images under investigation and a reference image (e.g. Nagler et al. 1998). Unfortunately, the images of July, that was intended as reference image for snowless conditions, was not available as a pair. The analysis of shadow and layover showed that great parts of the area of interest had to be excluded. Therefore, we decided not to use the SAR images in the first step, but include them in a later phase of the project.

4 METEOROLOGICAL OBSERVATIONS

The observational network for the project contains a set of four meteorological stations located in the Schneealpe area (Figure 5). These are three valley stations (Wasseralalm, 802m a.s.l., Karlgraben, 790m a.s.l. and Kalte Mürz, 1060m a.s.l.) and one station on the Schneealpe plateau (Schneealpe, 1735m a.s.l.). Rainfall and air temperature are monitored at all stations, windspeed and wind direction at two stations, but relative humidity and global (solar) radiation are only monitored at Karlgraben. All data are registered by data loggers on a half hourly basis. While all the stations are unattended, if possible, operation was checked on a biweekly basis. However, during winter, part of the stations are occasionally inaccessible due to avalanche hazard. The battery energy supply is therefore backed up by solar panels. The data so collected were postprocessed to take care of some of the measurement problems. These include systematic errors in precipitation due to wind induced catch deficit. This is particularly a problem for the mountain station (Schneealpe). Another problem was that the anemometer occasionally blocked as it froze, so zero wind speeds were registered. Finally, the solar radiation sensor was occasionally covered by snow and only registered minimum solar radiation values. These effects were largely removed by the postprocessing of the data.

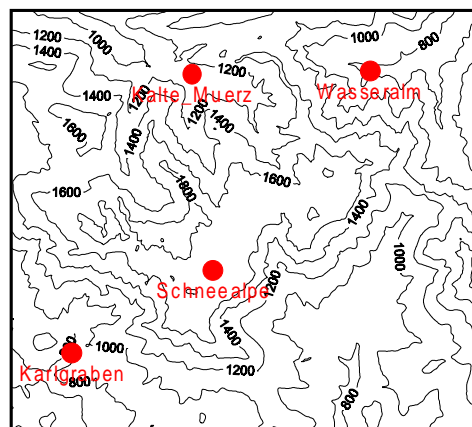


Figure 5: Topographic contours (m a.s.l.) and meteorological observation sites

5 HYDROLOGIC SNOW MELT MODEL

A snow accumulation and melt model was set up for the Schneealpe area based on the 20 m grid of the DTM. For each grid element the energy balance components at the snow surface were simulated and the coupled heat and mass flow within the snowpack was simulated by a multilayer point snow model (Blöschl and Kirnbauer, 1991). Atmospheric data used to drive the model include global (solar) radiation, air temperature, humidity, wind speed and precipitation on an hourly basis. These variables were observed at the meteorological stations and had to be interpolated to the model grid elements. Inputs of air temperature were assumed to decrease linearly with elevation based on the readings at the stations. Wind speed and relative humidity were taken as invariant across the catchment. The average catch deficit of the precipitation measurements was corrected by multiplying the precipitation readings by a snow correction factor. The energy balance components for each grid element were represented in the following way. Turbulent fluxes were estimated using a wind function. Long wave radiation was parameterised as a function of air temperature and humidity. Direct and diffuse solar radiation were estimated from observed solar radiation as a function of solar position, terrain aspect and slope which were computed from the DTM. Additionally, horizon shading of direct solar radiation was accounted for by making use of the sky plots. Snow surface albedo was assumed to decrease exponentially as a function of time after snowfall. The state of precipitation was determined as a function of air temperature (i.e. rainfall was

assumed to occur above a threshold air temperature and snowfall otherwise). One of the essential assumptions was how to represent the effects of wind drift. This was done by correcting snowfall for terrain effects by a wind drift factor F of the form

$$F = (a + b \cdot H) \cdot (1 - f(S)) \cdot (1 + e \cdot C) \geq 0$$

$$f(S) = \begin{cases} 0 & \dots S < c \\ \frac{S - c}{d - c} & \dots \text{otherwise} \end{cases}$$

where H is elevation, S is slope and C is terrain curvature at the grid scale of the digital elevation model. Based on previous experience with this approach (Blöschl et al., 1991) and a visual examination of the SPOT snow cover patterns (Figures 3 and 4) the parameters were set to $b=0.0001\text{m}^{-1}$, $c=10^\circ$, $d=60^\circ$ and $e=50\text{m}$, and a was estimated from the precipitation data and a mass balance condition within the simulation area.

For most of the model parameters, values from the literature were used. However, some of the parameters are likely to be site dependent and thus had to be calibrated. These parameters include snow albedo, the snow correction factor and the threshold air temperature. The calibration procedure involved simulating the snow cover patterns (i.e. areas of snow/no snow) and comparing these patterns with the SPOT derived snow cover images such as those in Figure 4. As mentioned above, the ground snow cover may be masked by snow free tree canopies and we therefore only compared pixels with low and/or sparse vegetation. Initially, the comparison indicated that, for these pixels, snow cover was generally overestimated by the snow model. We then reduced the albedo and increased the threshold temperature, and reran the snow model with these changed parameters. By matching simulated and SPOT derived snow cover images we obtained improved estimates of the model parameters in steps. Finally, a model parameter set was obtained that provided the best fit to the patterns.

6 RESULTS AND CONCLUSION

The grid based snow model with these parameters allowed us to simulate the snow accumulation and depletion processes during the snow cover period. The output of the model for each grid element and for each time step of 1 hour is: the snow water equivalent (i.e. the total mass of the snow pack in units mm); the snow melt intensity at the bottom of the pack in mm/h; the hydraulic state of the snow pack (i.e. how much liquid water is present in the pack, if any) expressed in terms of liquid water content (mm); and the thermal state of the snow pack (i.e. how deep the snow temperature is below zero, if at all) expressed in terms of cold content (mm).

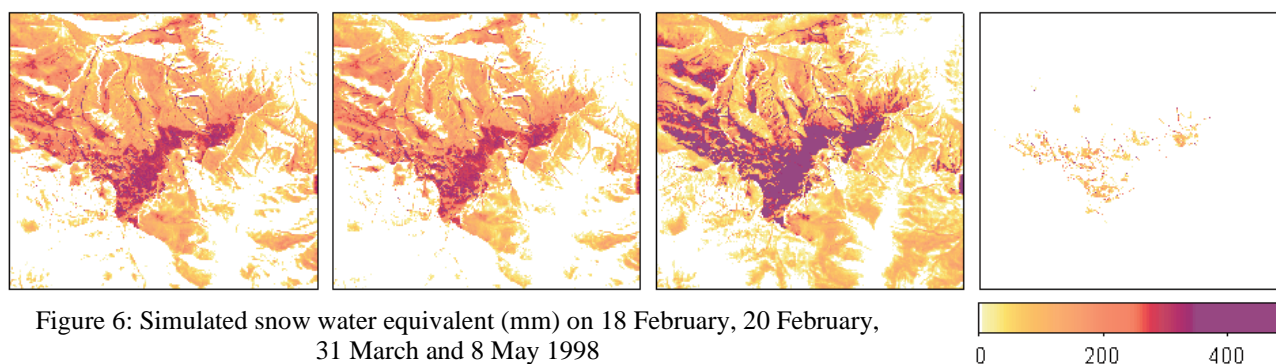


Figure 6: Simulated snow water equivalent (mm) on 18 February, 20 February, 31 March and 8 May 1998

Figure 6 shows the simulated snow water equivalent in the study area for the same dates as in Figure 3. In Figure 6, dark areas represent large values of the snow water equivalent and white areas represent snow free ground. On the Schneetalpe plateau in the centre of the images the snow water equivalent increases from 300mm in February to almost 500mm in March but decreases to a patchy snow cover of less than 100mm in May. In the valleys only a shallow snow cover is simulated in February, some snow in March and no snow in May. In addition to the effects of elevation, the snow water equivalent images in Figure 6 show patterns that are a reflection of wind drift with more snow in the gullies (note the thin dark bands in the top half of the images) as well as snow melt associated with solar radiation (note the earlier depletion of south facing slopes in the top half of the images for February 18 and 20).

It is interesting to compare these results with the SPOT images in Figure 3 and the snow classes in Figure 4. For the May image the simulated snow water equivalent roughly coincides with the SPOT images, and the same is true of the lower half of the February images. However, there has apparently been more snow simulated in the March image and in the top half of the February images than was classified from the SPOT data. As mentioned above, the model calibration has been based on pixels with low and/or sparse vegetation as these have been deemed to reliably reflect the true ground conditions. For these pixels, simulated snow water equivalent matches closely the SPOT derived snow cover patterns. It

is therefore likely that most of the discrepancies between Figures 6 and 3 are due to bare vegetation being visible in the SPOT images while in reality there may have been still some snow on the ground.

The simulated snow water equivalent can now be used for an assessment of the amount of snow that is available on the ground at any given point in space and time which can serve as a basis for management decisions associated with the operation of the water supply system. From an operational perspective one is also interested in the amount of melt water that leaves the snow pack as a function of time. Simulation results of snow melt, cumulated over time, have been plotted in Figure 7. The four lines represent snowmelt at the snow/ground interface (including rain on bare ground) averaged over the catchment areas of the four main water supply springs. It is interesting that in the catchment represented by the pink line, snow melt occurs earlier and more intense than in the other catchments. This is likely due to a number of reasons. The average elevation of this catchment is lower than that of the other catchments and the slopes are mainly south facing. This leads to earlier and more intense melt as a consequence of larger solar radiation inputs. Also, the catchment is essentially concave which leads to an above average accumulation of snow. Snow melt in the other catchments is quite similar which is a consequence of similarities in the topographic conditions.

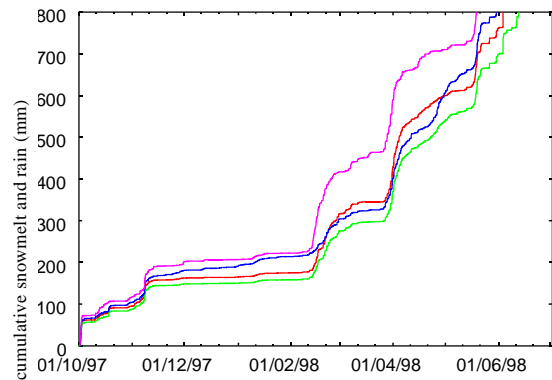


Figure 7: Simulated cumulative melt water production for four spring catchments

This study has shown that SPOT derived snow classifications are very useful for calibrating a hydrologic model of snow accumulation and depletion processes. With the calibrated model one can then obtain estimates of snow water equivalent and snow melt at any given point in time and space within the modelling domain. Future work will be directed towards more quantitatively incorporating ERS SAR based snow classifications into the modelling framework. We are also planning to represent snow interception in the vegetal canopy by an additional component of the snow model and to test the model more rigorously against additional ground data and satellite derived data.

ACKNOWLEDGEMENTS

The project "Schneealpe" has been supported through funding by the Austrian Federal Ministry of Science and Transport GZ 79083/2-III/A/5/98. The Water Management Department of Vienna made available funds for buying many of the SPOT images. ESA provided eight ERS2 SAR scenes in 1999 through project AO-123 within the framework of the Third Announcement of Opportunity.

REFERENCES

- Blöschl, G. and R. Kirnbauer, 1991. Point snowmelt models with different degrees of complexity - internal processes. *Journal of Hydrology*, 129, pp. 127-147.
- Blöschl, G., R. Kirnbauer and D. Gutknecht, 1991. Distributed snowmelt simulations in an Alpine catchment. 1. Model evaluation on the basis of snow cover patterns. *Water Resources Research*, 27 (12), pp. 3171-3179.
- Caves, R., Turpin, O., Clark C., Ferguson R., Quegan S., 1999. Comparison of Snow Covered Area Derived from Different Satellite Sensors: Implication for Hydrological Modelling. In: *Earth Observation: From Data to Information. Proceedings of the 25th Annual Conference and Exhibition for the Remote Sensing Society*, 8-10 September 1999, pp. 545-552.
- I.P.F. (Institute of Photogrammetry and Remote Sensing), Vienna University of Technology, 1999. Product Information SCOP at http://www.ipf.tuwien.ac.at/produktinfo/scop/englisch/scop_e.html (30 March 2000).
- Jensen J.R., 1996. *Introductory Digital Image Processing: A Remote Sensing Perspective*. 2 Edition. Prentice-Hall, NJ.
- Nagler T, H. Rott, G. Glendinning, 1998. SAR-based snow cover retrievals for runoff modelling. *Proc. of Second International Workshop on Retrieval of Bio- and Geophysical Parameters from SAR Data for Land Applications (ESTEC, Noordwijk, NL, Oct.1998)*, ESA SP-441, pp.511-517.
- Winther J.G., 1999. Satellite-derived Snow Coverage Related to Hydropower Production in Norway: Present and Future. *International Journal of Remote Sensing*, Vol. 20, No 15 and 16, pp 2991-3008.